RELATIONSHIP BETWEEN MICROSTRUCTURE, TENSILE DUCTILITY, AND FRACTURE TOUGHNESS OF Ti- AND Al-ALLOYS

C. Müller, A. Gysler, and G. Lütjering*

The influence of grain size and degree of age-hardening on the fracture behavior of Ti-8.6Al, Ti-6Al-4V, and Al-5.9Zn-2.6Mg-1.7Cu was investigated. It was found that the fracture toughness of these alloys can be affected by microstructural parameters in two different ways: by a direct influence on the fracture properties of the material, such as ductility, and by their influence on the geometry of crack extension and crack front. Crack propagation in the Ti- and Al-alloys occurred through microcrack nucleation ahead of the crack tip and subsequent connection with the main crack.

INTRODUCTION

The influence of grain size on fracture toughness of high strength alloys seems still not very satisfactory understood (1,2). Reductions in grain size usually are improving yield stress, uniaxial tensile ductility, and fatigue strength while the resistance against fatigue crack propagation normally is affected in the opposite way (3,4). However, such a clear pattern has not been established with regard to the grain size effect on fracture toughness. For high strength Al-alloys most experimental results indicate increased fracture toughness with grain refinements (2,5), while the results reported in the literature for Ti-alloys are still contradictory (1,6). Recent studies on defined microstructures of Ti-alloys showed a tendency for decreasing toughness with grain size reductions (7,8). The effect of age-hardening on fracture toughness is demonstrated in the literature in most cases

*Technische Universität Hamburg-Harburg,
2100 Hamburg 90, W.-Germany

by an inverse relationship between yield stress and fracture toughness (1,2,9), although the yield stress might not be the best parameter to describe the fracture behavior of a material.

The purpose of the present study was to investigate the effects of grain size and degree of age-hardening on fracture toughness of high strength Ti- and Al-alloys. The results are discussed with regard to the effects of these microstructural parameters on tensile ductility and on the geometry of crack extension and crack front in fracture toughness tests.

EXPERIMENTAL PROCEDURE

The tests were performed on three Ti-8.6Al alloys with oxygen contents of 500, 1000, and 2000 ppm (Timet), on Ti-6Al-4V (RMI), and on a Al-5.9 Zn-2.6Mg-1.7Cu alloy (Alcan), containing less than 0.01 % of each Cr, Fe, and Si (all compositions in wt.%). Equiaxed structures with different grain sizes or phase dimensions were prepared by thermomechanical processing from rolled plates, the details of these procedures are as previously published for Ti-8.6Al (10), Ti-6Al-4V (11), and for the Al-alloy (12). In addition fine and coarse lamellar structures were prepared for the Ti-6Al-4V alloy (8). It should be noted that the Ti-8.6Al alloy had a strong basal texture and the α-phase of equiaxed Ti-6Al-4V a mixed basal/transverse texture (11), due to the applied unidirectional rolling procedure. The lamellar structure of Ti-6Al-4V and the Al-alloy were nearly texture free.

All mechanical tests were performed at room temperature with the stress axis parallel to the rolling direction (equiaxed structures). Tensile tests were done on round samples with gage dimensions of 4 mm diameter and 20 mm length applying an initial strain rate of $10^{-3}s^{-1}$. The tensile properties, together with aging treatments and grain sizes, are summarized for the Ti-alloys in Table 1, and for the Al-alloy in Figure 8.

Fracture toughness tests were carried out (according to ASTM E-399) on CT-specimens with a thickness B of 8 mm and a width W of 32 mm. The fatigue pre-cracking (R=0.1, sine wave, 30 Hz) and the fracture toughness tests were performed in vacuum ($<10^{-4}$Pa) on a servohydraulic testing machine. The total notch length, including 4mm fatigue crack, was

TABLE 1 - Aging Treatment, Grain Size, and Tensile Properties

Alloy (wt.%)	Aging	Grain Size (μm)	$\sigma_{0.2}$ (MPa)	σ_F (MPa)	ε_F
Ti-8.6Al (1000 ppm O_2)	10 h 500°C	45	825	930	0.15
		110	755	815	0.09
	260 h 500°C	45	(920)	920	~ 0
		110	(835)	835	~ 0
Ti-6Al-4V					
equiaxed		2	1120	1650	0.62
		12	1045	1350	0.50
	24 h 500°C				
lamellar		2*	1045	1270	0.16
		12*	945	1090	0.13

* width of α phase

0.5 W. Monotonic loading was done at a rate of 1.7 $MPa \cdot m^{1/2} \cdot s^{-1}$. The load was monitored as a function of crack opening displacement, measured with a clip gage in front of the chevron notch.

The crack tip configuration in the center of CT specimens (plane strain region) was investigated by interrupting fracture toughness tests at defined K levels within the stable crack extension regime to determine the beginning of crack extension, and the crack geometry. These unloaded specimens were then sliced in the mid-thickness (0.5 B). Small samples containing the crack tips were polished and slightly etched to reveal the microstructure.

EXPERIMENTAL RESULTS

Titanium Alloys

The effect of age-hardening on fracture toughness of Ti-8.6Al is shown in Figure 1 for two different grain sizes. By increasing the degree of age-hardening the fracture toughness decreased, for example from 58 to 52 $MPa \cdot m^{1/2}$ by increasing the aging time at 500°C from 10 to 260 h (grain size 45 μm). The true tensile ductility ε_F decreased for the material with 45 μm grain size from 0.15 to a macroscopic value of 0 with increased age-hardening (Table 1).

The influence of oxygen on fracture toughness was investigated on Ti-8.6Al (grain size 110 μm) with 500 ppm and 2000 ppm oxygen, age-hardened for 24 h at 500°C (13). The results in Figure 2 showed that the fracture toughness decreased markedly from 60 to below 40 MPa·$m^{1/2}$ by increasing the oxygen content from 500 to 2000 ppm. The tensile ductility ε_F also exhibited a drastic loss from 0.4 to 0.05 by increasing the oxygen content from 500 to 2000 ppm (13).

The effect of grain size on fracture toughness for the Ti-8.6Al alloy also can be seen in Figure 1. The fracture toughness was higher for the coarse grained in comparison to the fine grained material for both age-hardening conditions. For example the toughness increased from 58 to 75 MPa·$m^{1/2}$ by increasing the grain size from 45 to 110 μm (age-hardened 10 h at 500°C). The influence of grain size on fracture toughness was also tested for a Ti-8.6Al alloy with a high oxygen content of 2000 ppm which was age-hardened for 100 h at 500°C. The results in Figure 3 showed that the grain size effect on fracture toughness for this alloy with a high oxygen content and a high degree of age-hardening was very small and exhibited even a slightly higher K_5 value for the smaller grain size (Figure 3).

Detailed studies of the crack tip configurations of these Ti-8.6 Al alloys revealed that crack advance occurred through the nucleation of microcracks along grain boundaries in the plastic zone ahead of the crack front and their subsequent connection with the main crack. Examples are shown in Figure 4 for Ti-8.6Al with grain sizes of 45 μm and 110 μm (1000 ppm oxygen, 10 h at 500°C). It can be seen that the distances between these microcracks were much shorter and the crack path was smoother for the fine grained in comparison to the coarse grained material (compare Figure 4a with b). It should be noted that variations in degree of age-hardening and in oxygen content for a constant grain size did not significantly change the geometry of the propagating crack.

The effect of phase dimensions on fracture toughness was investigated for fine and coarse equiaxed and fine and coarse lamellar microstructures of the (α+β) Ti-6Al-4V alloy. The equiaxed structures (Figure 5a) were prepared with α phase dimensions of 2 μm (fine) and 12 μm (coarse). The lamellar microstructures were also tested with two different α phase dimensions:

fine lamellar with 2 μm (Figure 5b) and coarse lamellar with 12 μm width of the α phase (Figure 5c). The length of the lamellae can be as long as the prior β grain size (several hundred μm).

The fracture toughness results for equiaxed and lamellar Ti-6Al-4V are shown in Figure 6. It can be seen that K_0, K_5 and K_{max} were higher for the coarse as compared to the fine equiaxed and lamellar microstructures. For example K_5 increased from 50 to 65 $MPa \cdot m^{1/2}$ by increasing the width of the α phase from 2 to 12 μm for the lamellar structure. Crack tip investigations exhibited a similar behavior as already described for the Ti-8.6Al alloy. Crack propagation occurred through nucleation of microcracks ahead of the crack front, mainly along α/β phase boundaries (8), and interconnection with the main crack. This mechanism again resulted in much smoother crack profiles for the fine microstructures (Figure 7a) due to shorter distances between the small cracks in comparison to the much more irregular crack path of the coarse structure (Figure 7b).

Aluminum Alloys

The effects of age-hardening and grain size on uniaxial tensile properties and on fracture toughness of the Al-alloy are summarized in Figure 8.

The tensile properties (upper part in Figure 8) exhibited the well known dependence on age-hardening and on grain size: a weak effect of grain size on $\sigma_{0.2}$ but a pronounced influence on ductility (12).

The effect of age-hardening on fracture toughness also showed the usually observed behavior: the highest values were found for the underaged, the lowest for the peakaged, and intermediate values for the overaged condition.

The effect of grain size on fracture toughness was not very pronounced. In the under- and peakaged conditions the coarser materials were slightly superior in comparison to the fine grained structures while almost no grain size effect on fracture toughness was observed for the overaged condition (Figure 8).

Investigations of the crack tips also showed that crack advance in all microstructures occurred by microcrack nucleation and subsequent connection with

the main crack. In the underaged condition crack extension took place through void nucleation and growth for the fine grain size, resulting in a dimple type of fracture surface (Figure 9a), while for the coarse microstructure a mixture of void nucleation and growth, and grain boundary fracture was found (Figure 9b). The peakaged condition exhibited crack nucleation at grain boundaries and subsequent fracture along grain boundaries for both grain sizes. The crack profile was much smoother for the fine grained (Figure 9c) in comparison to the coarse grained material (Figure 9d).

In the overaged condition crack propagation occurred through void nucleation for the fine grained microstructure resulting in a rather smooth fracture surface (Figure 9e). The coarse grained overaged condition exhibited portions of grain boundary fracture and dimple rupture (Figure 9f) and therefore showed a more irregular crack profile as compared to the fine microstructure.

DISCUSSION

Microstructural parameters can affect fracture toughness in two different ways: first through a direct influence on the fracture properties of the material (e.g. ductility) and second through their influence on the geometry of crack extension and crack front. In the alloys tested in this study crack propagation occurred through the nucleation of microcracks within the plastic zone ahead of the crack front and their subsequent connection with the main crack. The nucleation sites and distances of these small cracks had a pronounced influence on the geometry of the propagating cracks. In order to assess the effect of microstructure on ductility and in turn on fracture toughness it would be desirable to use ductility values obtained under plane strain condition. Since only preliminary plane strain tensile results were obtained so far the discussion will be based on uniaxial tensile ductility.

Titanium Alloys

Degree of age-hardening and oxygen content. These parameters will be discussed together since increasing oxygen content in Ti-alloys also increases the yield stress and lowers the ductility by promoting slip planarity, similar as increased age-hardening due to

Ti_3Al particles (14). The influence of increased age-hardening or oxygen level (grain size constant) on the geometry of crack extension in Ti-8.6Al was small. However, this increased age-hardening (Table 1) or oxygen level (13) resulted in a drastic loss in ductility. Therefore, it can be assumed that the observed decline in fracture toughness with increasing age-hardening and oxygen content (Figures 1 and 2) is dominated by the direct influence of these parameters on the ductility of the material.

Effect of grain size. The influence of grain or phase dimensions on the geometry of the propagating cracks was very pronounced (Figures 4 and 7). The distances between the observed microcracks at grain or α/β phase boundaries in the plastic zone were much shorter for the fine microstructures. The process of connecting these more closely spaced cracks with the main crack and the resulting smoother crack front is thought to explain the lower fracture toughness of the materials with fine grain or phase dimensions (Figures 1 and 6).

However, with decreasing grain size usually an increase in ductility can be observed (Table 1). This effect which tends to increase the fracture toughness is thought to be responsible for the decreasing differences between the fracture toughness values of fine and coarse grained materials with increasing degree of age-hardening or oxygen level (Figures 1 and 3). The alloy with the high oxygen level showed even a slightly better ranking of the fine grained material (Figure 3). The effect of ductility now apparently dominated over geometrical crack front effects.

Aluminium Alloys

Degree of age-hardening. In Al-alloys the effect of age-hardening on fracture toughness and on ductility is qualitatively very similar (15). Both curves are passing through a minimum in the peakaged condition (Figure 8). Therefore it seems realistic to assume that the influence of the variations in crack front geometry as a function of the age-hardening treatments used in this study on fracture toughness was small, similar as observed for the Ti-alloys.

Effect of grain size. The variations in crack front geometry with varying grain size were pronounced (Figure 9) and apparently almost counterbalanced the effect of variations in ductility with grain size on fracture toughness (Figure 8). This behavior is simi-

lar as already discussed for the Ti-8.6Al alloy (Figure 3) with a high degree of age-hardening (2000 ppm O_2, 100 h 500°C).

REFERENCES

(1) Stubbington, C.A., "Alloy Design for Fatigue and Fracture Resistance", AGARD-CP-185, 1976.

(2) Kaufman, J.G., "Alloy Design for Fatigue and Fracture Resistance", AGARD-CP-185, 1976.

(3) Lütjering, G. and Gysler, A.,"Aluminum Transformation Technology and Applications", ASM, Metals Park, 1980.

(4) Lütjering, G., Gysler, A., and Wagner, L., "Proceedings European Materials Society Conference", Strasbourg, France, 1985.

(5) Gräf, M., and Hornbogen, E., Acta Met., Vol. 25, 1977, pp. 883-889.

(6) Greenfield, M.A., and Margolin, H., Met. Trans., Vol. 2, 1971, pp. 841-847.

(7) Gysler, A., Bachmann, V., and Lütjering, G., "Fracture and the Role of Microstructure", EMAS, London, 1982.

(8) Gysler, A., and Lütjering, G., "Titanium Science and Technology", DGM, 1985.

(9) Paton, N.E., Williams, J.C., Chesnutt, J.C., and Thompson, A.W., "Alloy Design for Fatigue and Fracture", AGARD-CP-185, 1976.

(10) Lindigkeit, J., Terlinde, G., Gysler, A., and Lütjering, G., Acta Met., Vol. 27, 1979, pp.1717-1726.

(11) Peters, M., and Lütjering, G., "Titanium 80, Science and Technology", AIME, 1980.

(12) Lütjering, G., Hamajima, T., and Gysler, A., "Fracture 1977", University of Waterloo Press, 1977.

(13) Gray, G.T., and Lütjering, G., "Titanium Science and Technology", DGM, 1985.

(14) Williams, J.C., and Lütjering, G., "Titanium 80, Science and Technology", AIME, 1980.

(15) Ostermann, F., "Fortschritt-Berichte der VDI-Zeitschriften", VDI, Düsseldorf, 1975.

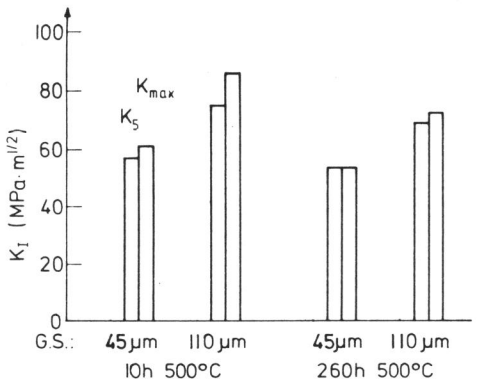

Ti-8.6Al, Vacuum

Figure 1 Influence of age-hardening and grain size on fracture toughness

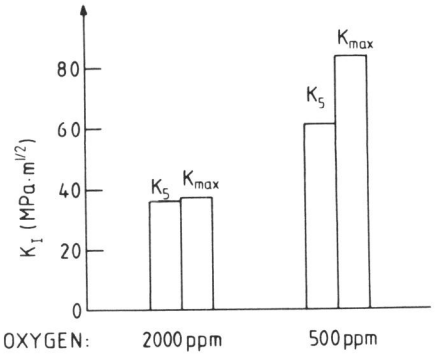

Ti-8.6Al, Vacuum

Figure 2 Influence of oxygen content on fracture toughness

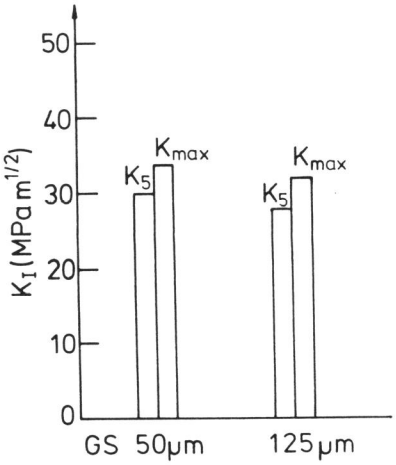

Ti-8.6Al, 2000 ppm O_2
100 h 500°C, Vacuum

Figure 3 Influence of grain size on fracture toughness

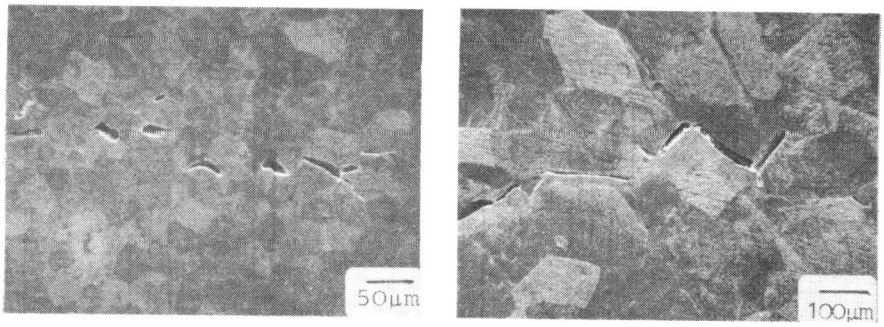

a) Grain size 45 µm b) Grain size 110 µm

Figure 4 Crack path in center of fracture toughness specimens, Ti-8.6Al, 10 h 500°C

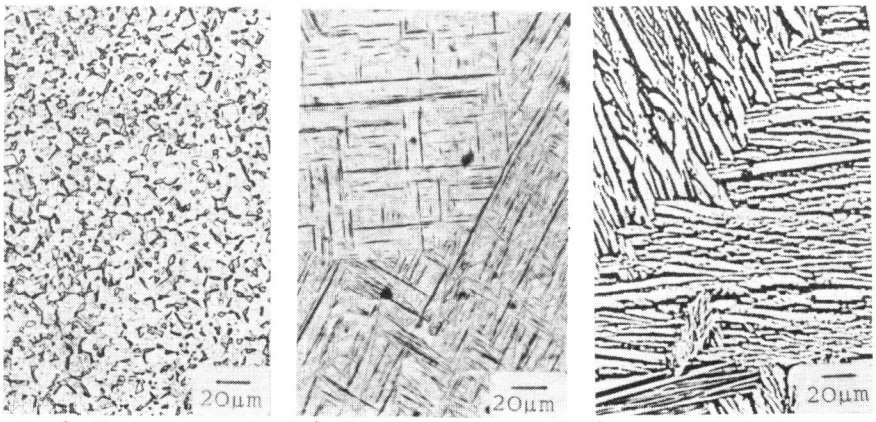

a) Equiaxed b) Fine lamellar c) Coarse lamellar

Figure 5 Geometrical arrangements of (α+β) structures of Ti-6Al-4V

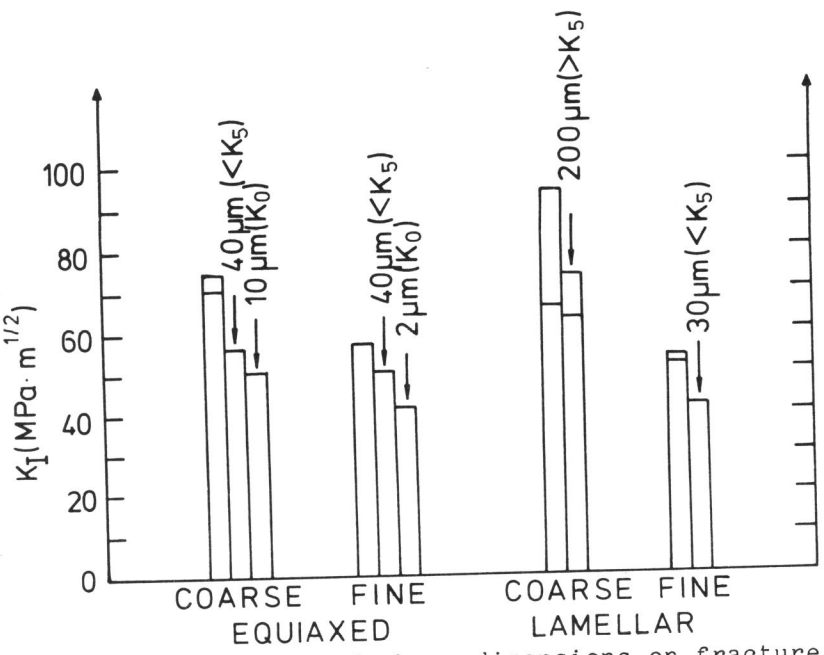

Figure 6 Influence of phase dimensions on fracture toughness, Ti-6Al-4V, 24h 500°C, Vacuum

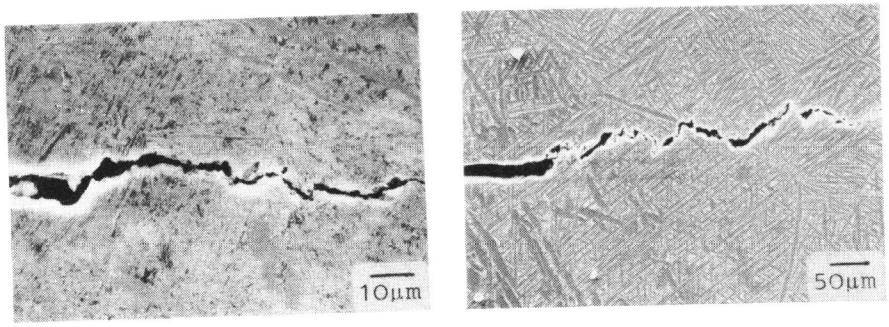

a) Fine lamellar b) Coarse lamellar

Figure 7 Crack path in center of Fracture toughness specimens, Ti-6Al-4V

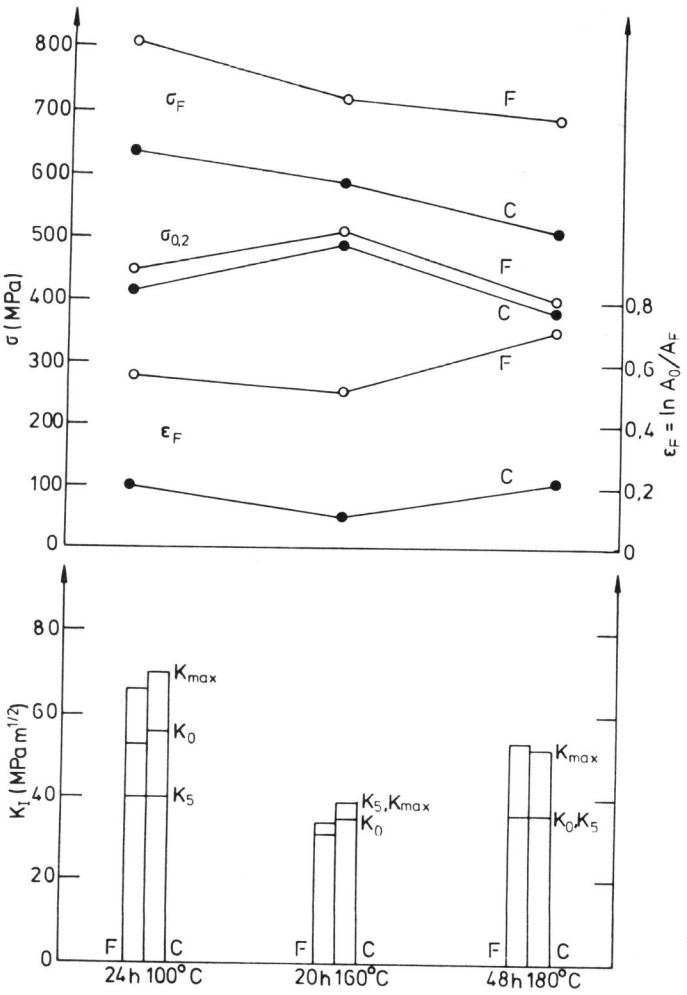

(F: grain size 50µm, C: grain size 300µm)
Al-5.9Zn-2.6Mg-1.7Cu, Vacuum

Figure 8 Influence of age-hardening and grain size on tensile properties and fracture toughness

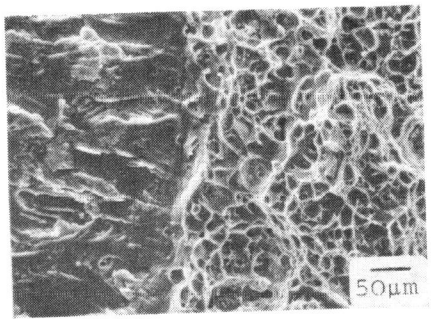

a) Grain size 50 µm
24 h 100°C

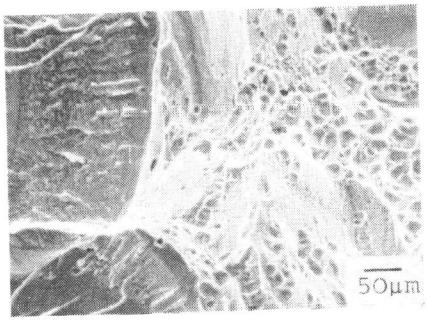

b) Grain size 300 µm
24 h 100°C

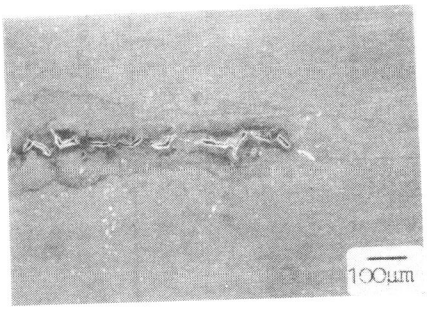

c) Grain size 50 µm
20 h 160°C

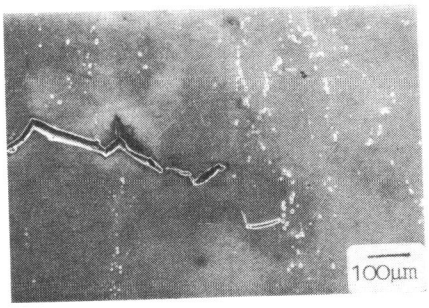

d) Grain size 300 µm
20 h 160°C

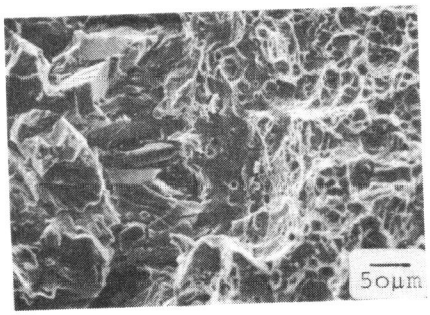

e) Grain size 50 µm
48 h 180°C

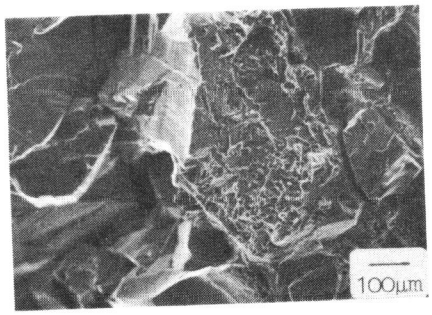

f) Grain size 300 µm
48 h 180°C

Figure 9 Fracture surfaces and crack path in center of fracture toughness specimens of Al-5.9Zn-2.6Mg-1.7Cu